Catalysis Today 176 (2011) 458–464

Contents lists available at ScienceDirect

Catalysis Today

journal homepage: www.elsevier.com/locate/cattod

Effect of vanadium dispersion and support properties on the catalytic activity of V-SBA-15 and V-MCF mesoporous materials prepared by direct synthesis

Marco Piumetti[a], Barbara Bonelli[a,*], Pascale Massiani[b], Stanislaw Dzwigaj[b], Ilenia Rossetti[c], Sandra Casale[b], Lucia Gaberova[b], Marco Armandi[a], Edoardo Garrone[a]

[a] Department of Materials Science and Chemical Engineering, INSTM Unit Torino Politecnico, Politecnico di Torino, Corso Duca degli Abruzzi 24, 10129 Turin, Italy
[b] UPMC, Université Pierre et Marie Curie (Paris VI), CNRS-UMR 7197, Laboratoire de Réactivité de Surface, 4 place Jussieu, F-75005 Paris, France
[c] Dipartimento di Chimica fisica ed Elettrochimica, ISTM-CNR and INSTM Unit, Università degli Studi di Milano, via C. Golgi 19, 20133 Milano, Italy

ARTICLE INFO

Article history:
Available online 19 November 2010

Keywords:
Vanadium
V-SBA-15
V-MCF
Dichloromethane oxidation
Chlorinated volatile organic compounds (Cl-VOCs)

ABSTRACT

Two V-SBA-15 and V-MCF materials (V content *ca.* 2.5 wt.%) were prepared by direct synthesis and tested in the catalytic decomposition of dichloromethane. Their catalytic properties were compared to those of other materials with the same vanadium content, namely two mesoporous materials prepared by impregnation (V-SBA-15-i and V-MCF-i) and a non-porous one prepared by flame pyrolysis (V-SiO_2). Both direct synthesis and flame pyrolysis methods allowed a better vanadium dispersion that lead to better catalytic properties above 350 °C, due to the presence of well dispersed V species partially incorporated into silica. The higher dichloromethane conversion achieved with both V-SBA-15 and V-SBA-15-i samples, as compared to MCF samples, are ascribed to longer residence times of both reactants and products within SBA-15 mesoporous channels, in contrast to three-dimensional MCF ultra large pores facilitating diffusion. Below 350 °C, both V-SBA-15-i and V-MCF-i samples showed higher dichloromethane conversion, basically due to the presence of micro-crystalline V_2O_5 formed at the external surface of both materials.

1. Introduction

Chlorinated volatile organic compounds (Cl-VOCs) are used as solvents in many industrial processes, although they are often toxic/carcinogenic substances and contribute to atmospheric pollution [1–3]. During the last years, several technologies have been developed in order to reduce their environmental release, such as adsorption/absorption processes; photocatalytic degradation; hydrodechlorination and thermal incineration. Among the latter, adsorption/absorption methods are often not applicable on an industrial scale, whereas high temperature incineration produces other very toxic compounds, *e.g.* dioxins, NO_x, etc. Therefore, catalytic oxidation would be an interesting solution for Cl-VOCs abatement, making possible their decomposition at relatively low temperatures (*e.g.* 200–500 °C) [4–7].

Both supported noble metals [8,9] and metal oxides [10,11] are currently employed for the total oxidation of hazardous organic air pollutants: the former, though more active, are too expensive and undergo deactivation by chlorinated compounds in gas stream [8]; the latter, though not expensive, are by far less active. All this notwithstanding, literature reports that vanadium-based catalysts are effective towards the catalytic oxidation of several volatile organic compounds [12–15]. V-containing mesoporous silicas (*e.g.* V-SBA-15, V-MCM-41, V-MCM-48, V-MCF, etc.) with uniform pores size and high surface area are interesting catalysts for oxidation reactions, allowing a large concentration of accessible and well defined active centres (VO_x), often incorporated into the silica framework [16–20]. Although such catalysts are usually prepared by impregnation, it has been observed that V-SBA-15 materials prepared by direct synthesis exhibit larger surface area, better dispersion and reducibility of V species and superior catalytic performances in both selective and total oxidation reactions [17,18]. In the present paper, the effect is studied of both vanadium dispersion (isolated V species *versus* micro-crystalline V_2O_5) and support properties (surface area, structure, etc.) on the catalytic oxidation of dichloromethane (CH_2Cl_2), the most stable chlorinated-alkane. Two V-containing mesoporous silicas (V-SBA-15 and V-MCF), with *ca.* 2.5 wt.% V content, were prepared by direct synthesis and tested in the CH_2Cl_2 decomposition, used as a probe reaction for Cl-VOCs total oxidation. The relation between the physico-chemical properties and catalytic performance of such materials was investigated in relation to other catalysts with comparable vanadium content, namely (i) two impregnated samples (V-SBA-15-i and V-MCF-i) and (ii) a non-porous sample (V-SiO_2) prepared by flame pyrolysis (FP),

* Corresponding author. Tel.: +39 011 5644719; fax: +39 011 5644699.
E-mail address: barbara.bonelli@polito.it (B. Bonelli).

0920-5861/$ – see front matter © 2010 Elsevier B.V. All rights reserved.
doi:10.1016/j.cattod.2010.10.066

a high temperature synthesis technique allowing a good vanadium dispersion to be achieved [21].

2. Experimental

2.1. Catalysts synthesis

V-SBA-15 sample (vanadium content about 2.5 wt.%) was prepared as reported in the literature [17,18]. SBA-15 silica obtained by following the same recipe [18], except for the addition of vanadium, was used both as blank-sample and as support of impregnated sample V-SBA-15-i. V-MCF sample (vanadium content about 2.5 wt.%) was obtained by direct synthesis, as reported earlier [19]: 4.0 g $EO_{20}PO_{70}EO_{20}$ (Pluronic P123, Sigma–Aldrich) and 2.0 g 1,3,5-trimethylbenzene (TMB, Sigma–Aldrich) as organic swelling agent were dissolved in 30.0 mL water and stirred at room temperature for 5 h. Afterwards, 9.0 g tetraethylorthosilicate (TEOS, Sigma–Aldrich) and a proper amount of ammonium metavanadate (NH_4VO_3, Sigma–Aldrich) were added to the solution. In order to obtain isolated V species incorporated into the silica framework, 0.20 M HCl was added drop-wise to the solution until pH reached a value close to 3.0, as reported in literature [20]. After stirring at 40 °C for 24 h at constant pH, the solution was transferred into a Teflon autoclave and aged at 100 °C for 24 h. The sample was then filtered off, washed with bi-distilled water and dried overnight at 100 °C under static conditions. Finally, the included surfactant was removed by calcination at 600 °C for 5 h in air. Two catalysts (V-SBA-15-i and V-MCF-i) were obtained by impregnation with NH_4VO_3 solution of SBA-15 and MCF supports, respectively, followed by drying and calcination at 600 °C in air. A non-porous catalyst (V-SiO_2) was prepared by flame pyrolysis (FP) method [21].

2.2. Catalysts characterization

The main textural properties of all the prepared samples were obtained as follows: (i) BET (Brunauer–Emmett–Teller) specific surface area (S_{BET}) was measured by N_2 adsorption/desorption isotherms at −196 °C on *ca.* 30 mg sample previously outgassed at 150 °C for 5 h to remove molecular water and other atmospheric contaminants (Quantachrome Autosorb 1); (ii) Pores Size Distributions (PSDs) were calculated by either applying the Barrett–Joyner–Halenda (BJH) algorithm to isotherms desorption branch (SBA-15 materials) or according to the modified Broekhoff de Boer (BdB) method using Hill's approximation for the adsorbed layer thickness (MCF materials) [22]; (iii) powders X-ray diffraction (XRD) patterns were collected on a Philips PW3040 diffractometer, using Cu Kα radiation (2θ range = 0.8–10°; step = 0.02° 2θ; time per step: 1 s).

Samples morphology was studied by Transmission Electron Microscopy (TEM, JEM 2011 operating at 200 kV); V-content was determined by EDS analysis (Oxford 7353 probe on a LEO 1450 VP microscope): for each sample, 5 different spots with a 10–50 nm diameter, were selected in representative zones of the sample, and then an average V-content was calculated. For H_2-TPR (Temperature Programmed Reduction) experiments, *ca.* 100 mg sample was placed in a quartz micro-reactor, then contacted with reducing flowing gas (5% molar H_2 in Ar, 40 mL min^{-1}) and heated in the 20–1000 °C temperature range (heating rate: 10 °C min^{-1}), while recording H_2 consumption using a Thermal Conductivity Detector (TCD); a gas condenser operated at −196 °C and placed prior the TCD was used to remove water possibly formed by reduction.

Micro-Raman spectra were collected at ambient conditions on a Renishaw micro-Raman system, equipped with an Ar laser (514.5 nm). For infrared (IR) measurements, powder samples were pressed into thin, self-supporting wafers and pre-treated under high vacuum (residual pressure <10^{-3} mbar) using a standard vacuum frame, in a quartz cell equipped with KBr windows. Fourier Transform IR (FT-IR) spectra were collected at 2 cm^{-1} resolution on a Bruker Equinox 55 FTIR spectrophotometer, equipped with a MCT detector. To study surface dehydroxylation, samples were outgassed for 1 h at 150 and 500 °C before collecting IR spectra. To study surface acidic properties, ammonia was dosed at room temperature on samples outgassed at 150 and 500 °C: in a typical experiment, increasing pressures of ammonia (0.01–20 mbar range) were dosed on each sample and adsorption reversibility was checked by prolonged evacuation (about 30 min) at room temperature.

2.3. Catalytic activity

Catalytic tests were carried out in a continuous quartz tubular reactor (7 mm i.d.) heated by an electric furnace, as reported elsewhere [18]. In a typical experiment, *ca.* 70 mg catalyst was activated before each run in air (flowing rate: 41 mL min^{-1}) at 500 °C for 1 h. The gas flow was then switched from air to the reactive mixture (1000 ppm CH_2Cl_2 in air, VVH = 21,000 h^{-1}) and catalytic activity was investigated in the 200–500 °C temperature range. The outlet gas composition was analyzed by an on-line gas chromatograph (PERICHROM, PR 2100) with two detection lines: the former, for analysis of organic compounds, was equipped with a capillary column and a flame ionization detector (FID); the latter, for CO_x detection, was equipped with a succession of a Porapak-Q (for backflush) and a MS-5A columns, and a thermal conductivity detector (TCD). The percentage of dichloromethane conversion was calculated as moles of CH_2Cl_2 converted over moles of CH_2Cl_2 fed. The selectivity to each *i*th product was calculated as ratio of moles of *i*th product over moles of converted CH_2Cl_2, normalized to the respective stoichiometric coefficients.

3. Results and discussion

3.1. Catalytic activity in CH_2Cl_2 decomposition

Fig. 1a and b reports the main catalytic results for the CH_2Cl_2 oxidative decomposition in the 200–500 °C temperature range and Table 1 reports both conversion and selectivity values measured at 500 °C. Pure silica SBA-15 was tested as blank sample, showing no conversion (not reported) [18]. As a whole, all the catalysts showed: (i) stable conversions in the explored temperatures range (maximum reaction time tested = 2 h); (ii) almost constant conversion and selectivity values, in that after reaction the samples were reactivated at 500 °C and several reaction–reactivation cycles were repeated: the obtained data were completely reproducible. In agreement with literature [23,24], Cl-containing by-products were mostly HCl, the most thermodynamically favoured compound at high temperature, and, to a minor extent, Cl_2, but only at low temperatures.

Fig. 1a shows that conversion increases with increasing temperature in all cases, but the following differences are observed from

Table 1
Dichloromethane conversion (%) and CO_2 selectivity (%) obtained with V-SBA-15, V-SBA-15-i, V-MCF, V-MCF-i and V-SiO_2 catalysts during catalytic tests under aerobic conditions at 500 °C.

Sample	CH_2Cl_2 conversion (%)	CO_2* selectivity (%)
V-SBA-15	68	95
V-SBA-15-i	31	48
V-MCF	52	75
V-MCF-i	23	45
V-SiO_2	43	65

* CO_2 was the only product measured in aerobic conditions with our experimental set up; the "missing products" could involve coke and/or adsorbed compounds.

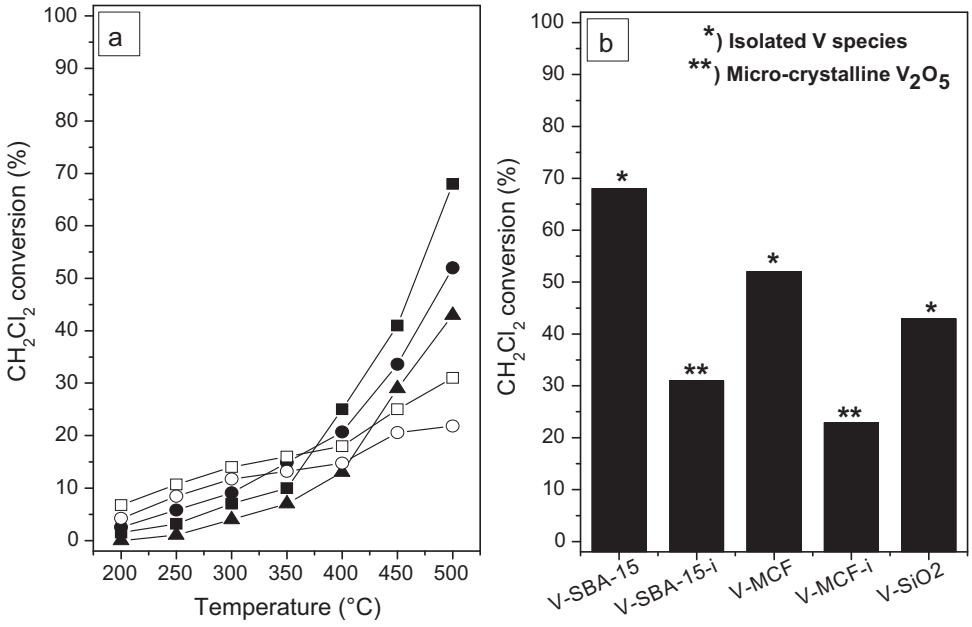

Fig. 1. (a) Dichloromethane conversion as a function of temperature under aerobic conditions over samples V-SBA-15 (■), V-MCF (●), V-SBA-15-i (□), V-MCF-i (○) and V-SiO_2 (▲). (b) Conversion values measured at 500 °C under aerobic conditions over the same catalysts; t = 10 min.

sample to sample: (i) above 350 °C (Fig. 1a), the two most active catalysts are V-SBA-15 and V-MCF, respectively, with CH_2Cl_2 conversions at 500 °C (Fig. 1b) that are approximately twice those of impregnated catalysts (V-SBA-15-i and V-MCF-i, respectively); (ii) V-SBA-15 and V-MCF show both higher conversion and selectivity to CO_2 than V-SBA-15-i and V-MCF-i (Table 1); (iii) above 400 °C, the non-porous V-SiO_2 sample, with highly dispersed V species incorporated into the silica framework [21], exhibits higher CH_2Cl_2 conversions than V-SBA-15-i and V-MCF-i; (iv) below 350 °C, both V-SBA-15-i and V-MCF-i materials give slightly higher conversions.

As shown in Fig. 1, above 350 °C V-SBA-15 gave higher conversions than V-MCF, and, similarly, higher CH_2Cl_2 conversions were obtained with V-SBA-15-i rather than with V-MCF-i. Such findings seem to be related to different diffusion phenomena occurring inside the porous structure of the two systems studied. In principle, the structure of mesocellular silica foams (MCFs), featuring a three-dimensional network with large pores (15–20 nm), should favour molecules diffusion, unlike mesoporous channels of SBA-15, occurring in one dimension only. Reactants and products can be much more retained within mesopores of SBA-15 as compared to ultra-large pores of three-dimensional MCF systems: such a longer residence time could favour deeper oxidation with both V-SBA-15 and V-SBA-15-i catalysts.

Besides that, catalytic properties may be influenced by both (i) different vanadium dispersion, depending on the synthesis procedure; (ii) different support properties, like hydrophilicity/hydrophobicity and (iii) acidic properties, as discussed below.

3.2. Effect of vanadium dispersion on the catalytic activity

Micro-Raman spectra of all the samples studied are reported in Fig. 2a: V-SBA-15, V-MCF and V-SiO_2 spectra show a band at 1030–1035 cm^{-1} due to V=O groups belonging to mono-vanadates species drawn in Scheme 1, indicating the presence of isolated V species incorporated inside silica walls; both V-SBA-15 and V-SiO_2 spectra show other bands due to the presence hydrated poly-vanadates (520, 690, 920 and 1020 cm^{-1}); with both V-SBA-15-i and V-MCF-i samples, additional bands are seen at 408, 550, 732, and 990 cm^{-1}, the latter being more intense, corresponding to the presence of micro-crystalline V_2O_5 [18,29]. H_2-TPR analysis is reported in Fig. 2b: V-SBA-15, V-MCF and V-SiO_2 TPR profiles show only one maximum at *ca.* 560 °C, readily assigned to the reduction of isolated (or at least low polymeric) V species, whereas both V-SBA-15-i and V-MCF-i profiles exhibit additional reduction peaks at higher temperatures (in the 600–800 °C range), due to the presence of micro-crystalline V_2O_5 that is typically reduced above 650 °C [18,19]. Fig. 3 reports TEM images of the samples studied: (i) with both V-SBA-15 and V-SBA-15-i samples, well-ordered arrays of mesoporous channels are observed (Figs. 3a and b, respectively) in agreement with SBA-15 hexagonal structure, confirmed by XRD patterns reported in Fig. 4. With V-SBA-15-i, however, few aggregates are observed (inset to Fig. 3b), readily assigned to the presence of VO_x species at the external surface of particles; (ii) V-SiO_2 (Fig. 3c) shows amorphous nanoparticles of variable dimensions without evidence of any segregation of vanadium oxide; (iii) both V-MCF and V-MCF-i samples (Figs. 3d and e, respectively) show a disordered array of 3D mesoporous spherical cells (*ca.* 20–25 nm in diameter) typical of MCF. The measured cell sizes are in fair agreement with pore sizes determined from N_2 isotherms (Table 2). Similarly to V-SBA-15-i, V-MCF-i sample (Fig. 3e) shows also the presence of several VO_x clusters (dotted box) (Fig. 3e). Fig. 4 reports XRD patterns of V-SBA-15 and V-SBA-15-i samples, along with those of SBA-15 silica, reported for comparison [18]: all patterns in the figure show a main diffraction peak due to $d_{(100)}$ reflection of SBA-15 hexagonal space group $p6mm$, the corresponding inter-reticular distances (d_0) and unit cell parameters ($a_0 = 2d_0/\sqrt{3}$) being reported in Table 2. At higher 2θ angles, $d_{(110)}$ and $d_{(200)}$ reflections are not observed, indicating that the adopted synthesis procedure leads to less ordered materials than traditional SBA-15, as observed previously [18]. As reported in Table 2, V-SBA-15-i has almost the same unit cell parameter value of parent SBA-15 silica, confirming that V may not enter silica walls by impregnation, whereas V-SBA-15 has a larger a_0 probably due to vanadium entering silica walls [18].

In summary, V-SBA-15, V-MCF and V-SiO_2 samples mainly show isolated V species incorporated into silica walls, whereas with both V-SBA-15-i and V-MCF-i either VO_x or micro-crystalline V_2O_5 are present at their external surface [18,19]. Such micro-crystalline V_2O_5 may interact with CH_2Cl_2 molecules, even at low temperatures, since mass-transfer limitations are avoided at the external

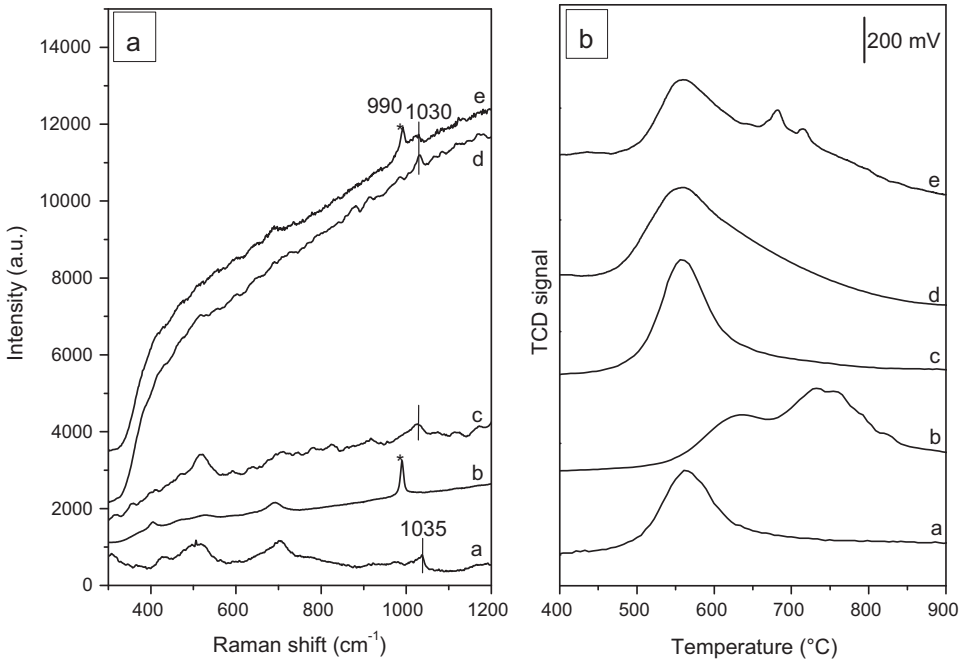

Fig. 2. Raman spectra (Section a) and H_2-TPR profiles (Section b) of samples V-SBA-15 (a), V-SBA-15-i (b), V-SiO_2 (c), V-MCF (d) and V-MCF-i (e).

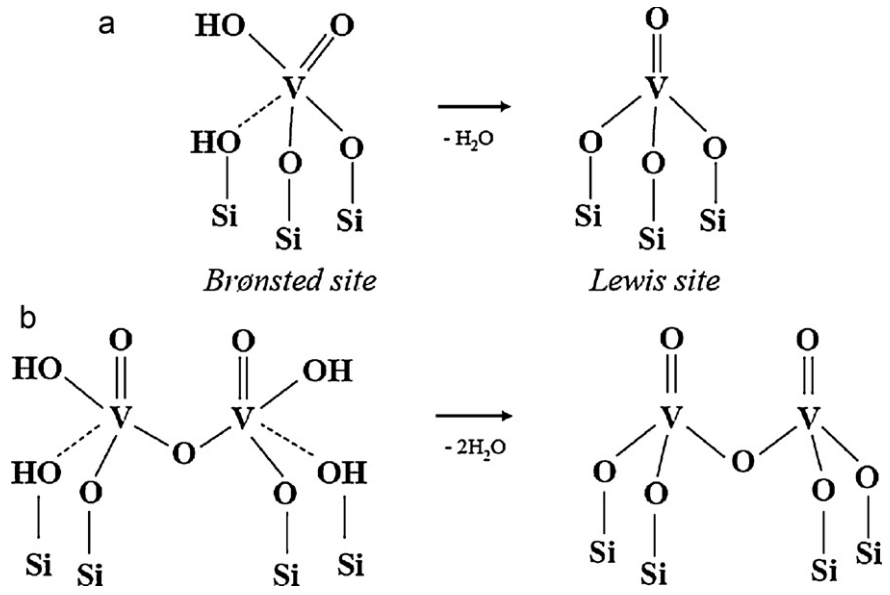

Scheme 1. Dehydroxylation mechanism proposed for highly dispersed V-containing silica materials: (a) monovanadate species and (b) dimeric VO_x species.

Table 2
Textural properties of the prepared samples as derived from both N_2 isotherms at −196 °C and XRD patterns.

Sample	Synthesis method	Reference	V-content (wt.%)[a]	S_{BET} ($m^2\ g^{-1}$)	D (nm)	d_0 (nm)[e]	a_0 (nm)[f]
SBA-15	Direct	[18]	–	630	3.3[b]	6.7	7.7
V-SBA-15	Direct synthesis	[18]	2.4	820	3.5[b]	7.4	8.6
V-SBA-15-i	Impregnation	[18]	2.8	530	3.5[b]	6.7	7.8
V-MCF	Direct synthesis	[19]	2.6	925	16[c]; 6[d]	–	–
V-MCF-i	Impregnation	[19]	2.5	645	23[c]; 12[d]	–	–
V-SiO_2	Flame pyrolysis	[21]	3.0	40	-	–	–

[a] As measured by EDS analysis on 10–50 nm spots chosen in representative zones of the sample.
[b] Mesopores diameter as calculated according to the BJH method from isotherms desorption branch.
[c] Cells diameter as determined from adsorption branches of N_2 isotherms (BdB–FHH method).
[d] Windows diameter as determined from desorption branches of N_2 isotherms (BdB–FHH method).
[e] d_0 = inter-reticular distance.
[f] a_0 = cell parameter as calculated from $a_0 = 2d_0/\sqrt{3}$.

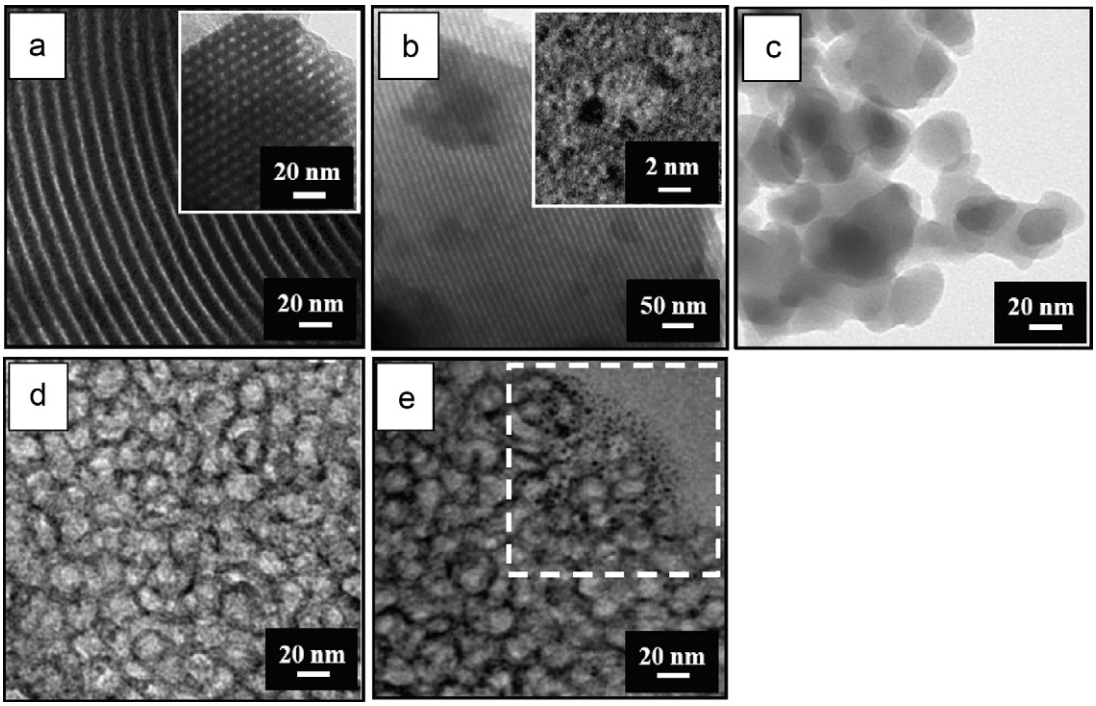

Fig. 3. TEM images of samples: V-SBA-15 (a); V-SBA-15-i (b); V-SiO_2 (c); V-MCF (d) and V-MCF-i (e).

surface of particles. As far as the presence of vanadium oxide is concerned, the Brønsted acidic properties of micro-crystalline V_2O_5 are known to play a role on catalytic activity at low temperature [18]: several authors, indeed, proposed that strong Brønsted acidic sites, like those at the surface of micro-crystalline V_2O_5, act as preferential adsorption sites of Cl-VOCs during the first oxidation step [14].

Furthermore, the catalytic performances of the V-SiO_2 sample are slightly worse than those of V-MCF and V-SBA-15, although V-SiO_2 shows highly dispersed V species, as well. This is probably due to the lower surface area of V-SiO_2 as compared to the other mesoporous samples (Table 2).

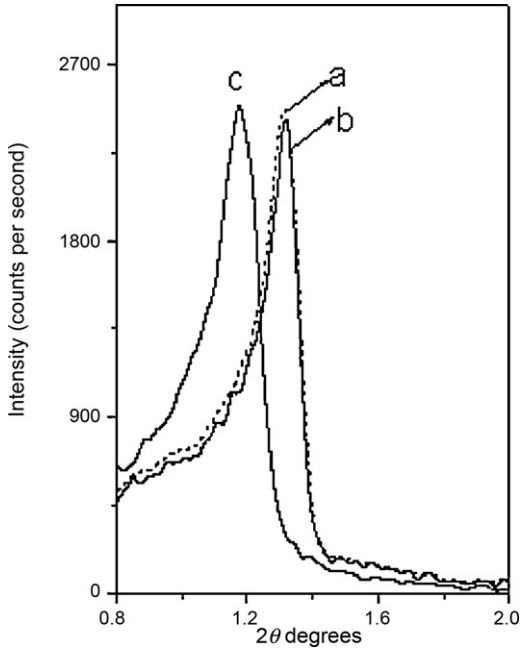

Fig. 4. Powders XRD patterns of: SBA-15 (dotted curve a); V-SBA-15-i (curve b) and V-SBA-15 (curve c).

3.3. *Effect of the support hydrophilic/hydrophobic properties and acidity on the catalytic activity*

Catalysts hydrophobic/hydrophilic properties are known to have an influence on the catalytic activity in oxidation reactions [23]. For example, water molecules produced during oxidation processes may reduce the effectiveness of active centres: this effect is particularly evident with more hydrophilic materials and at lower temperatures [23,25].

For this reason, samples were outgassed at 150 and 500 °C in order to study their hydroxyls population and dehydration behaviour above and below 350 °C, the temperature at which a change occurs in the catalytic behaviour of the studied materials. Fig. 5a and b compares IR spectra in the hydroxyls range (3800–3000 cm^{-1}) of samples outgassed at 150 and 500 °C, respectively. All IR spectra were normalized to unit specific weight, to allow comparison. IR spectra of the samples outgassed at 150 °C are different from sample to sample, but all of them show basically two absorption bands: the former at 3740–3745 cm^{-1} is due to isolated silanols [18,26], whereas the broader and intense absorption on the lower wave numbers side is due to H-bonded hydroxyls [18,26].

The intensity of H-bonded silanols signal is smaller with both impregnated samples, V-SBA-15-i (curve b) and V-MCF-i (curve e): this can be related to their smaller surface area with respect to samples prepared by direct synthesis, but also to the fact that impregnation occurs at the expenses of H-bonded species, which are more reactive than isolated silanols [26]. With V-SiO_2 sample (curve c), bands due to free silanols (3745 cm^{-1}) and H-bonded silanols appear, as well [21,26]. The relatively high concentration of H-bonded silanols, given its lower surface area, was previously assigned to the formation of a metastable oxide at high temperature [21]: the FP-method leads, indeed, to materials in which V species are partly incorporated in the silica framework and the rapid dehy-

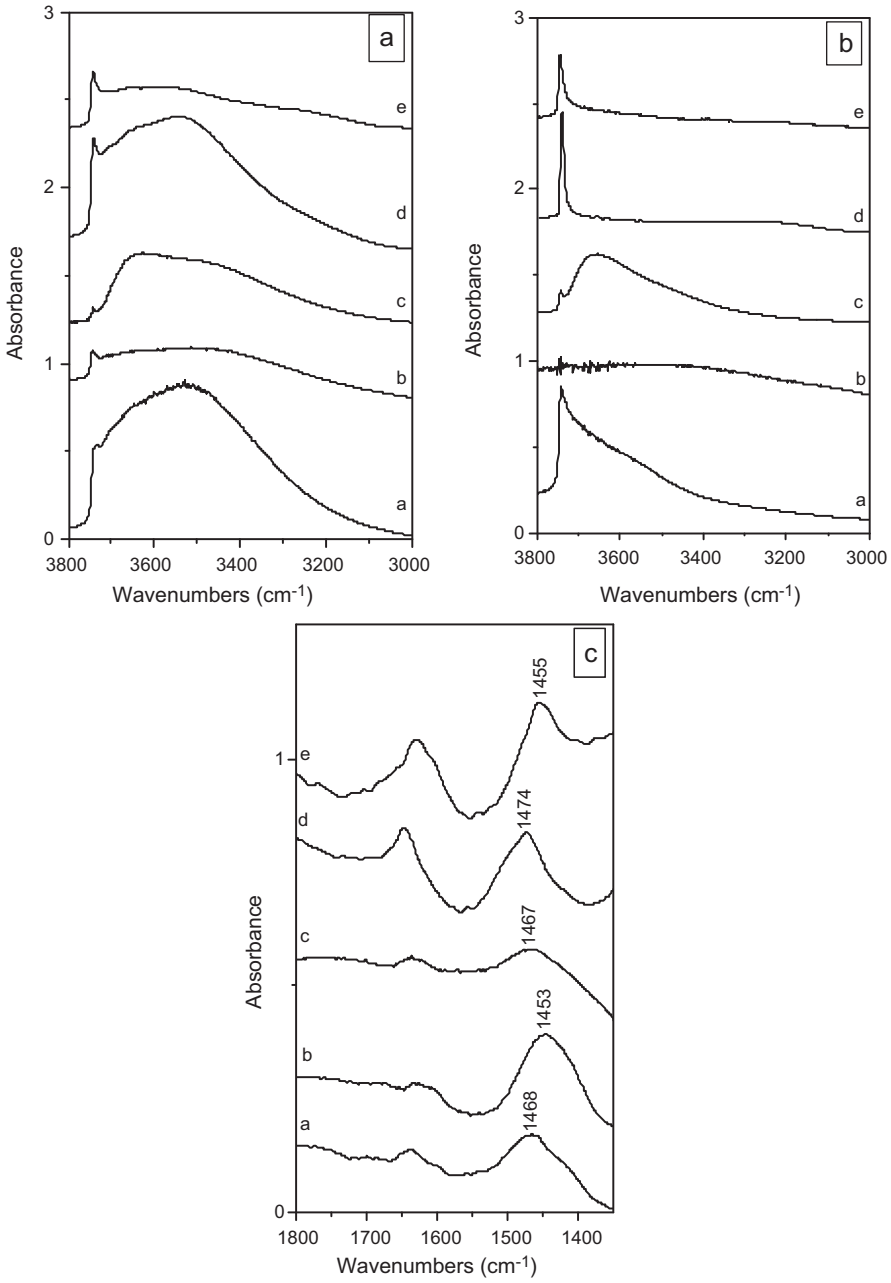

Fig. 5. IR spectra, in the 3800–3000 cm^{-1} range, of samples: V-SBA-15 (a); V-SBA-15-i (b); V-SiO_2 (c); V-MCF (d); V-MCF-i (e) outgassed at 150 °C (Section a) and 500 °C (Section b). IR spectra recorded after dosing *ca.* 1.0 mbar NH_3 on the samples outgassed at 150 °C (Section c).

dration forces the structure to adopt V–O–Si and Si–O–Si strained bonds, which are rapidly hydrolyzed during cooling in wet air. The V–OH stretching mode, expected *ca.* 3660 cm^{-1} according to the literature, is not observable in bare spectra because of extensive H-bonding [18,19,21], but evidence of their presence will be given by adsorption of ammonia discussed below.

Fig. 5b reports IR spectra of samples outgassed at 500 °C: as a whole, severe dehydroxylation occurs, as expected due to the temperature of the treatment, but the following considerations can be drawn: (i) MCF samples (curves d and e) show a very sharp band at 3745 cm^{-1}, due to the presence of (residual) isolated silanols, only, indicating that, *ceteribus paribus*, dehydroxylation is favoured by their three dimensional porous network, and no signals ascribable to either H-bonded hydroxyls or heterogeneous silanols population were observed; (ii) with V-SiO_2, beside that of isolated silanols, a hill-defined band is seen, previously assigned to intra-particles defective hydroxyls [21]; (iii) V-SBA-15 spectrum shows a band at 3745 cm^{-1} with a tail on the lower wave numbers side, due to the occurrence of a heterogeneous hydroxyls population, whereas sample V-SBA-15-i after outgassing at 500 °C shows negligible hydroxyls population and loss of transparency: its colour indeed turned to dark-green likely indicating reduction of microcrystalline V_2O_5 [26], in agreement with its TPR profile.

As a whole, the richer hydroxyl population, *i.e.* higher hydrophilicity, of materials prepared by both direct synthesis and FP may also explain their lower catalytic activity at low temperatures (below 350 °C). On the other hand, such samples should also show a high concentration of V–OH species that are known to behave as Brønsted acidic sites [18,19,21,27]. The latter, being highly dispersed inside the silica framework can be more easily converted into Lewis acidic sites by dehydroxylation (Scheme 1), playing a key role on the catalytic activity at higher temperatures.

Fig. 5c reports IR spectra registered after dosing *ca.* 1.0 mbar NH_3 on the samples previously outgassed at 150 °C: the bands with maxima in the 1468–1453 cm^{-1} range are due to the bending vibration of NH_4^+ species formed upon reaction between ammonia molecules and Brønsted hydroxyls [28,29]: with both impregnated samples, the band of ammonium is more intense, indicating a higher abundance of Brønsted hydroxyls (V–OH species). Furthermore, the blue shift of such band with respect to that of free ammonium ion (1410 cm^{-1}) can be used as a qualitative measure of the Brønsted acidic strength: the smaller blue shift observed with impregnated samples indicates that stronger Brønsted sites are likely obtained by impregnation. Additional bands in the 1650–1600 cm^{-1} range are assigned to: (i) ammonia molecules H-bonded to silanols (1635 cm^{-1}) and (ii) ammonia molecules adsorbed through the lone-pair to Lewis acidic sites (V^{5+} ions, band at 1613 cm^{-1}) [18,21]. The latter band is clearly seen with impregnated samples, confirming the presence of surface vanadium oxide. After adsorption of ammonia on samples outgassed at 500 °C (not shown), only bands due to ammonia molecules interacting with silanols and with Lewis acidic sites are observed, indicating that V–OH species were removed.

4. Conclusion

The set of catalysts studied show different catalytic activity in the explored temperature range: above 350 °C, V-SBA-15, V-MCF and V-SiO_2 catalysts gave higher conversions, due to the presence of isolated V-species incorporated inside silica walls. Comparison of dichloromethane conversions at 500 °C shows that both V-SBA-15 and V-SBA-15-i are more active than V-MCF and V-MCF-i, respectively: this behaviour is assigned to the different porous network of the two materials. With SBA-15 structure, monodimensional mesoporous channels may favour longer residence times of molecules, unlike the three-dimensional ultra-large pores of MCF and therefore deeper oxidations occur in SBA-15 materials.

Below 350 °C, both V-SBA-15-i and V-MCF-i samples were more active towards dichloromethane oxidation, due to the presence of micro-crystalline V_2O_5, which is more active at lower temperatures. Finally, the two impregnated catalysts showed a smaller hydroxyl population and a higher Brønsted acidity (due to VO_x clusters at the surface) that may also contribute to improve their catalytic activity at low temperatures.

References

[1] H. Sidebottom, J. Franklin, Pure Appl. Chem. 68 (1996) 1757.
[2] A. McCulloch, M.L. Aucott, T.E. Graedel, G. Kleiman, P.M. Midgley, Y.-F. Li, J. Geophys. Res. 104 (1999) 8417.
[3] S.H. Taylor, Top. Catal. 52 (2009) 457.
[4] K. Everaert, J. Baeyens, J. Hazard Mater. 109 (2004) 113.
[5] J.J. Spivey, Ind. Eng. Chem. Res. 26 (1987) 2165.
[6] C. Gennequin, S. Siffert, R. Cousin, A. Aboukaïs, Top. Catal. 52 (2009) 482.
[7] L. Pinard, J. Mijoin, P. Magnoux, M. Guisnet, J. Catal. 215 (2003) 234.
[8] H.L. Tidahy, S. Siffert, F. Wyrwalski, J.F. Lamonier, A. Aboukaïs, Catal. Today 119 (2007) 317.
[9] C. Gennequin, M. Lamallem, R. Cousin, S. Siffert, F. Aïssi, A. Aboukaïs, Catal. Today 122 (2007) 301.
[10] S. Ordonez, L. Bello, H. Sastre, R. Rosal, F.V. Diez, Appl. Catal. B: Environ. 38 (2002) 139–149.
[11] C. Lahousse, A. Bernier, P. Grange, B. Delmon, P. Papaefthimiou, T. Loannides, X. Verykios, J. Catal. 178 (1998) 214.
[12] J. Jones, J.R.H. Ross, Catal. Today 35 (1997) 97.
[13] S. Krishnamoorthy, J.P. Baker, M.D. Amiridis, Catal. Today 40 (1998) 39.
[14] R. Delaigle, D.P. Debecker, F. Bertinchamps, E.M. Gaigneaux, Top. Catal. 52 (2009) 501.
[15] F. Bertinchamps, M. Treinen, P. Eloy, A.M. Dos Santos, M.M. Mestdagh, E.M. Gaigneaux, Appl. Catal. B: Environ. 70 (2007) 360.
[16] F. Cavani, N. Ballarini, A. Cericola, Catal. Today 127 (2007) 113.
[17] F. Ying, J. Li, C. Huang, W. Weng, H. Wan, Catal. Lett. 115 (2007) 137.
[18] M. Piumetti, B. Bonelli, M. Armandi, L. Gaberova, S. Casale, P. Massiani, E. Garrone, Micropor. Mesopor. Mater. 133 (2010) 36.
[19] M. Piumetti, B. Bonelli, P. Massiani, Y. Millot, S. Dzwigaj, M. Armandi, L. Gaberova, E. Garrone, Micropor. Mesopor. Mater. 2010, in press.
[20] F. Gao, Y. Zhang, H. Wan, Y. Kong, X. Wu, L. Dong, B. Li, Yi Chen, Micropor. Mesopor. Mater. 110 (2008) 508.
[21] I. Rossetti, L. Fabbrini, N. Ballarini, F. Cavani, A. Cericola, B. Bonelli, M. Piumetti, E. Garrone, H. Dyrbeck, E.A. Blekkan, L. Forni, J. Catal. 256 (2008) 45.
[22] W.J. Lukens, P. Schmidt-Winkel, D. Zhao, J. Feng, G.D. Stucky, Langmuir 15 (1999) 5403.
[23] G. Ertl, H. Knözinger, F. Schüth, J. Weitkamp, page 2397 of Handbook of Heterogeneous Catalysis, 2nd ed., Wiley, John & Sons, Incorporated, 2008.
[24] J. Haber, T. Machej, M. Derewiński, R. Janik, J. Kryściak, H. Sadowska, J. Janas, Catal. Today 54 (1999) 47.
[25] A. Taguchi, F. Schüth, Micropor. Mesopor. Mater. 77 (2005) 1.
[26] B.A. Morrow, A.J. McFarlan, J. Phys. Chem. 96 (1992) 1395.
[27] S. Dzwigaj, E.L. El Malki, M.J. Peltre, P. Massiani, A. Davidson, M. Che, Top. Catal. 11/12 (2000) 379.
[28] A. Zecchina, L. Marchese, S. Bordiga, C. Pazè, E. Gianotti, J. Phys. Chem. B 101 (1997) 10128.
[29] M. Armandi, B. Bonelli, I. Bottero, C.O. Areán, E. Garrone, J. Phys. Chem. C 114 (2010) 6658, and references therein.